

# RSC Advances



This is an *Accepted Manuscript*, which has been through the Royal Society of Chemistry peer review process and has been accepted for publication.

*Accepted Manuscripts* are published online shortly after acceptance, before technical editing, formatting and proof reading. Using this free service, authors can make their results available to the community, in citable form, before we publish the edited article. This *Accepted Manuscript* will be replaced by the edited, formatted and paginated article as soon as this is available.

You can find more information about *Accepted Manuscripts* in the [Information for Authors](#).

Please note that technical editing may introduce minor changes to the text and/or graphics, which may alter content. The journal's standard [Terms & Conditions](#) and the [Ethical guidelines](#) still apply. In no event shall the Royal Society of Chemistry be held responsible for any errors or omissions in this *Accepted Manuscript* or any consequences arising from the use of any information it contains.

## High-performance flexible photodetectors based on single-crystalline Sb<sub>2</sub>Se<sub>3</sub> nanowires

Yao Liang,<sup>\*a</sup> Yingying Wang,<sup>b</sup> Jianan Wang,<sup>a</sup> Sumei Wu,<sup>a</sup> Dayong Jiang<sup>\*c</sup> and Jiabiao Lian<sup>\*d</sup>

<sup>a</sup>School of Materials Science and Engineering, Dalian Jiaotong University, Dalian 116028, P. R. China. E-mail: yliang0625@hotmail.com

<sup>b</sup>Department of Optoelectronic Science, Harbin Institute of Technology at Weihai, Weihai 264209, P. R. China.

<sup>c</sup>School of Materials Science and Engineering, Changchun University of Science and Technology, Changchun 130022, P. R. China. E-mail: dayongjiangcust@126.com

<sup>d</sup>School of Civil and Environmental Engineering, College of Engineering, Nanyang Technological University, Singapore 639798. E-mail: jblian@ntu.edu.sg

Antimony selenide (Sb<sub>2</sub>Se<sub>3</sub>) has many potential applications in photoelectric devices, thermoelectric cooling devices and electrochemical devices *etc.* It also has many special properties due to its layered structure. A simple hydrothermal method was used to synthesize Sb<sub>2</sub>Se<sub>3</sub> nanowires of high crystalline quality. (Sb<sub>4</sub>Se<sub>6</sub>)<sub>n</sub> layers are parallel to the growth direction of Sb<sub>2</sub>Se<sub>3</sub> nanowire. A single Sb<sub>2</sub>Se<sub>3</sub> nanowire demonstrated a remarkable response to 635 nm light at 10 V with the responsivity and external quantum efficiency of 360 A/W and 7.0×10<sup>4</sup> %, respectively. The rise/fall time was 0.4/1.3 s. Flexible photodetectors were fabricated by dispersing a large number of Sb<sub>2</sub>Se<sub>3</sub> nanowires onto the Au interdigitated electrodes on PET substrates, which showed fast response speed with the rise/fall time as low as 13/20 ms and excellent flexibility. The high-performance of photodetectors may be partially attributed to the layered structure. Generally, high-yield Sb<sub>2</sub>Se<sub>3</sub> nanowires synthesized by the hydrothermal method are promising candidates for high-performance flexible photodetectors.

## Introduction

Photodetectors are widely used in military and civil fields, such as binary switches, optical communications, flame sensors and missile detectors.<sup>1,2</sup> In the last decade, one-dimensional (1D) semiconductor nanostructures have demonstrated their potential as the functional parts in photodetectors due to large surface-to-volume ratio and high crystalline quality. Wide band-gap nanomaterials, such as ZnS nanowires, ZnO nanorods, WO<sub>3</sub> nanowires, TiO<sub>2</sub> nanotubes, In<sub>2</sub>Ge<sub>2</sub>O<sub>7</sub> nanowires and Zn<sub>2</sub>GeO<sub>4</sub> nanowires, have been investigated for UV-light detection.<sup>3-8</sup> Ge nanowires, In<sub>2</sub>Se<sub>3</sub> nanowires, CdSe nanowires, ZrS<sub>2</sub> nanobelts, Zn<sub>3</sub>P<sub>2</sub> nanowires, ZrSe<sub>3</sub> nanobelts, HfSe<sub>3</sub> nanobelts, InP nanowires, GaP nanowires *etc.* have exhibited their promise in fabricating visible-light photodetectors.<sup>9-15</sup> These reports confirm that photodetectors made from 1D nanostructures usually possess desirable performances, including high responsivity ( $R_\lambda$ ), fast response speed and excellent stability. Recently, flexible electronics have attracted more attention because of the need for portable devices.<sup>16-19</sup> Compared to thin film and bulk materials, 1D nanostructures can be assembled easily into flexible electronics with high bending stability due to their large bending strain compliance.<sup>20-23</sup>

Sb<sub>2</sub>Se<sub>3</sub> as an important member of group V-VI binary semiconductors can be used to fabricate electric, photoelectric, thermoelectric cooling and electrochemical devices, which is attributed to its direct and narrow band-gap, high environmental stability and Seebeck coefficient.<sup>24-27</sup> It is a highly anisotropic semiconductor with the layered structure parallel to the [001] (c-axis) direction.<sup>28,29</sup> Sb<sub>2</sub>Se<sub>3</sub> have demonstrated

promise in solar cells due to its layered structure.<sup>30</sup> Thus, it can be believed that single-crystalline  $\text{Sb}_2\text{Se}_3$  nanowires have many special properties owing to the carrier and photon confinement in the layered structure.<sup>29</sup>  $\text{Sb}_2\text{Se}_3$  nanowires have been synthesized by hydrothermal/solvothermal routes or microwave-assisted methods.<sup>25,28,31</sup> However, the studies on the application of  $\text{Sb}_2\text{Se}_3$  nanowires are limited. Zhai *et al.* utilized individual  $\text{Sb}_2\text{Se}_3$  nanowire to fabricate a photodetector with a marked response to 600 nm visible-light.<sup>29</sup> Choi *et al.* also studied the response of single  $\text{Sb}_2\text{Se}_3$  nanowire to 655 nm visible-light.<sup>27</sup> The photodetectors based on  $\text{Sb}_2\text{Se}_3$  nanowire films displayed a remarkable response to white light.<sup>31</sup> The results above indicate that  $\text{Sb}_2\text{Se}_3$  nanowires have bright prospects for visible-light photodetectors. However, these  $\text{Sb}_2\text{Se}_3$  nanowire based photodetectors were fabricated on the rigid  $\text{SiO}_2/\text{Si}$  substrates, which do not meet the need for portable devices. To the best of our knowledge, the application of  $\text{Sb}_2\text{Se}_3$  nanowires in flexible electronics has not been explored. Thus, it is necessary to further investigate the electrical transport and photoelectric properties of single  $\text{Sb}_2\text{Se}_3$  nanowire, assemble a large number of nanowires into the flexible photodetector, and finally characterize its performances. It is desirable to achieve high-performance flexible photodetectors *via* a simple method.

In this work, a simple hydrothermal method was used to synthesize single-crystalline  $\text{Sb}_2\text{Se}_3$  nanowires in high yields. Single  $\text{Sb}_2\text{Se}_3$  nanowire field-effect transistors (FETs) demonstrated the p-type transport characteristic of single nanowire. They were also utilized to investigate the photoelectric properties of single  $\text{Sb}_2\text{Se}_3$

nanowire. A single  $\text{Sb}_2\text{Se}_3$  nanowire showed a remarkable response to 635 nm light at 10 V with high responsivity (360 A/W) and short response time (0.4/1.3 s). Flexible photodetectors with fast response speed (13/20 ms) and excellent flexibility were made by dispersing a large number of  $\text{Sb}_2\text{Se}_3$  nanowires onto the Au interdigitated electrodes on PET substrates, revealing the potential application of  $\text{Sb}_2\text{Se}_3$  nanowires in flexible photodetectors.

## Experimental section

### Synthesis and characterization of $\text{Sb}_2\text{Se}_3$ nanowires

$\text{Sb}_2\text{Se}_3$  nanowires were synthesized by a template-free hydrothermal route.<sup>28</sup> 0.01 g  $\text{Sb}(\text{AcO})_3$ , 0.0085 g  $\text{Na}_2\text{SeO}_3$  and 0.3 ml hydrazine hydrate (80 wt%) were dissolved to 25 ml distilled water and the reaction solution was transferred into a 30 ml autoclave. Then, the autoclave was kept at 120 °C for 24 h. The synthesized product was characterized by scanning electron microscopy (SEM, QF400) equipped with an energy-dispersive X-ray (EDX) spectroscopy and high-resolution transmission electron microscopy (HRTEM, JEM 2100F).

### Electrical and photoelectric measurements of single $\text{Sb}_2\text{Se}_3$ nanowire

To investigate the electrical and photoelectric properties of single  $\text{Sb}_2\text{Se}_3$  nanowire, single nanowire based FETs were fabricated. Nanowires were dispersed into ethanol and then transferred onto  $\text{p}^+\text{-Si}$  substrates covered with a 150 nm  $\text{SiO}_2$  layer. The source and drain electrodes (Cr/Au 20/100 nm) were attached onto two terminals of a single  $\text{Sb}_2\text{Se}_3$  nanowire by e-beam lithography, resist development, metal deposition

and liftoff processes. The thin Cr layer serves as the adhesion layer to improve the adhesion of electrodes. Metal Al as the gate electrode was deposited on the back of Si substrate. FETs were characterized by using an electrometer (Keithley 6517A) to record  $I_{DS}$ - $V_{DS}$  curves at different gate voltages. To investigate the responses of a single nanowire to light,  $I_{DS}$ - $V_{DS}$  curves were measured under the illumination of 635 nm light with different power densities without a gate voltage. Its time responses were measured by the electrometer *via* periodically turning 635 nm light on-off.

### **Fabrication and characterization of flexible photodetectors**

Flexible photodetectors based on a large number of  $\text{Sb}_2\text{Se}_3$  nanowires were fabricated by dispersing nanowires onto the Au interdigitated electrodes on flexible PET substrates. The adhesion between the Au film and the PET substrate is good. The adhesion layer is not required. Thus, only the Au film was deposited as the electrodes. The interdigitated electrodes were made by Au deposition, photolithography, resist development, etching. Each electrode is composed of fifteen fingers with a width of 5  $\mu\text{m}$ , a length of 500  $\mu\text{m}$  and an interspacing of 5  $\mu\text{m}$ . The responses of photodetectors to visible-light were measured by a sourcemeter (Keithley 2635B).

## Results and discussion

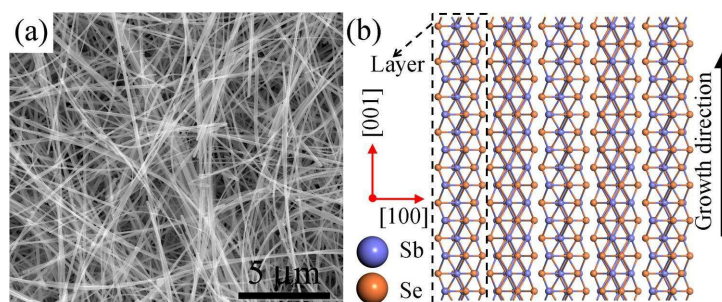


**Fig. 1** (a) SEM image of  $\text{Sb}_2\text{Se}_3$  nanowires. (b) Crystalline structure of  $\text{Sb}_2\text{Se}_3$ .  $(\text{Sb}_4\text{Se}_6)_n$  layers are parallel to the growth direction of  $\text{Sb}_2\text{Se}_3$  nanowire.

Fig. 1a shows an SEM image of the synthesized product, revealing that the product is composed of a large number of ultralong  $\text{Sb}_2\text{Se}_3$  nanowires. Their length is up to tens of microns.  $\text{Sb}_2\text{Se}_3$  nanowires have a diameter of about 100 nm and a smooth surface. An EDX spectrum was taken from the synthesized product (Fig. S1), showing that the product includes elements Sb and Se with an atomic ratio of 2:3. The morphology and crystalline structure of  $\text{Sb}_2\text{Se}_3$  nanowires were further characterized by HRTEM. Fig. S2(a) demonstrates a typical  $\text{Sb}_2\text{Se}_3$  nanowire with a uniform diameter of 98 nm along the growth direction and a smooth surface. Fig. S2(b) shows the HRTEM image and corresponding selected area electron diffraction (SAED) pattern of the nanowire, confirming that the  $\text{Sb}_2\text{Se}_3$  nanowire is of the orthorhombic structure and it is a single crystal, free from dislocations and grows along the [001] direction. The  $(\text{Sb}_4\text{Se}_6)_n$  layer parallel to the [001] direction is the basic unit of  $\text{Sb}_2\text{Se}_3$ .  $\text{Sb}_2\text{Se}_3$  nanowires are also composed of the  $(\text{Sb}_4\text{Se}_6)_n$  layers stacking parallel to the

growth direction of the nanowires, as shown in Fig. 1b. Carriers can be confined in the layered structure and transport efficiently along nanowires.<sup>30</sup>

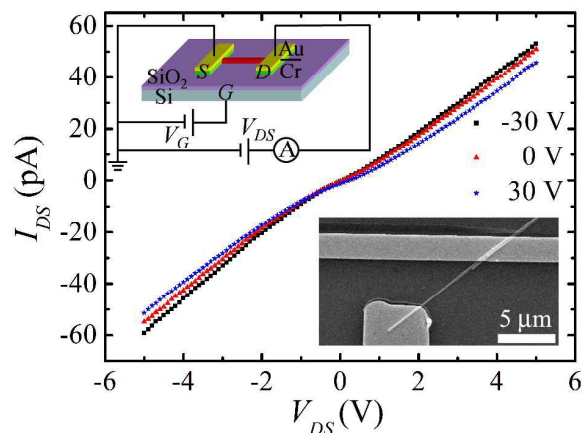


**Fig. 2**  $I_{DS}$ - $V_{DS}$  characteristics of a single  $\text{Sb}_2\text{Se}_3$  nanowire FET at different  $V_G$ . Insets are a schematic illustration and an SEM image of the FET, respectively.

Single  $\text{Sb}_2\text{Se}_3$  nanowire based FETs were fabricated to investigate the electrical transport properties of single nanowire. The upper inset in Fig. 2 is a schematic illustration of the FET. The lower inset in Fig. 2 is an SEM image of the FET, showing that two Cr/Au electrodes are attached onto a single  $\text{Sb}_2\text{Se}_3$  nanowire. The FET's channel is about  $6.4 \mu\text{m}$  in length and  $135 \text{ nm}$  in width. Fig. 2 displays  $I_{DS}$  versus  $V_{DS}$  curves at a different back-gated voltage ( $V_G$ ) varying from  $-30 \text{ V}$  to  $30 \text{ V}$ . The nonlinear  $I_{DS}$ - $V_{DS}$  curves indicate Schottky contacts between the nanowire and Cr/Au electrodes. The conductance of the  $\text{Sb}_2\text{Se}_3$  nanowire decreases with the increasing of positive  $V_G$ , proving that the nanowire is p-type. Compared to bulk materials, nanomaterials could have different electrical transport properties due to

large surface-to-volume ratio.  $\text{Sb}_2\text{Se}_3$  in bulk is well-known p-type semiconductor.<sup>25</sup>

Here,  $\text{Sb}_2\text{Se}_3$  nanowires have the same conductivity type as the bulk.

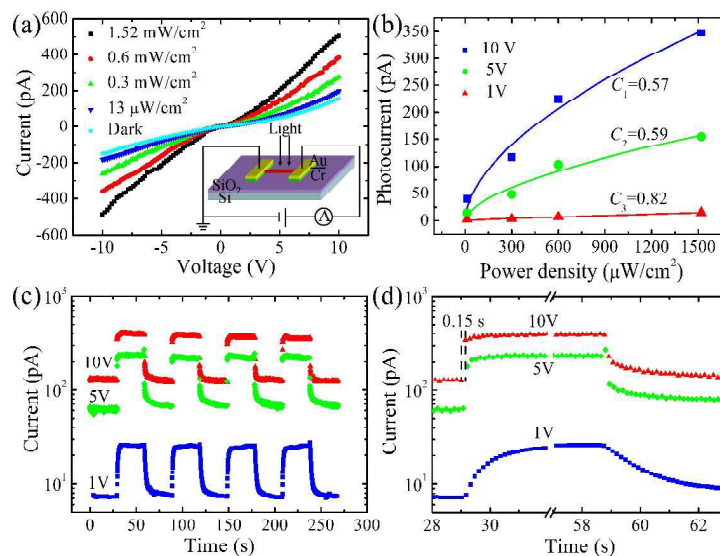


**Fig. 3** (a)  $I$ - $V$  curves of the  $\text{Sb}_2\text{Se}_3$  nanowire in the dark and under the 635 nm light illumination. Inset is a schematic illustration of measurement. (b) The relationships between photocurrent and power density at different biases. (c,d) The time responses to 635 nm light with the powder density of 1.52  $\text{mW}/\text{cm}^2$  at 1 V, 5 V and 10 V, respectively.

In the previous report,<sup>25</sup> the band-gap energy of  $\text{Sb}_2\text{Se}_3$  nanowires have been examined by UV-vis absorption spectra and derived to range from 1.16 to 1.17 eV, indicating that  $\text{Sb}_2\text{Se}_3$  nanowires can detect all visible-light in principle. The photoelectric properties of the  $\text{Sb}_2\text{Se}_3$  nanowire, shown in the lower inset of Fig. 2, were investigated. The inset of Fig. 3a is a schematic illustration of photoelectric measurement. Fig. 3a demonstrates  $I$ - $V$  curves of the nanowire in the dark and under

the 635 nm light illumination of different power densities. The photocurrent ( $I_{\text{light}}-I_{\text{dark}}$ ) increases with the increasing of the power density of incident light at a fixed bias. It is clear that the nanowire is sensitive to 635 nm light. The energy of incident photons is 1.95 eV, which is larger than the band-gap energy of  $\text{Sb}_2\text{Se}_3$ . Under the illumination of 635 nm light, electron-hole pairs are generated in the  $\text{Sb}_2\text{Se}_3$  nanowire, which leads to the increase of the conductivity of the nanowire.

Responsivity ( $R_\lambda = I_{ph}/(PS)$ , where  $I_{ph}$  is photocurrent,  $P$  is the power density of incident light and  $S$  is the effective illuminated area) and external quantum efficiency ( $EQE = hcR_\lambda/(e\lambda)$ , where  $\lambda$  is the wavelength,  $h$  is Planck's constant,  $e$  is the electronic charge and  $c$  is the speed of light) are important parameters representing the sensitivity of photodetector.<sup>32</sup> The single  $\text{Sb}_2\text{Se}_3$  nanowire photodetector has  $R_\lambda$  and  $EQE$  as high as 360 A/W and  $7.0 \times 10^4$  % respectively at a bias of 10 V (The calculation is shown in the supporting information). The  $R_\lambda$  is higher than that ( $R_\lambda = 8.0$  A/W) of the single  $\text{Sb}_2\text{Se}_3$  nanowire photodetector reported by Zhai *et al.* and comparable to that ( $R_\lambda = 560$  A/W) reported by Choi *et al.*<sup>27,29</sup> It can be concluded that  $\text{Sb}_2\text{Se}_3$  nanowires synthesized by this hydrothermal method have a potential application in visible-light detection. The higher  $R_\lambda$  and  $EQE$  are attributed to excellent crystalline quality of  $\text{Sb}_2\text{Se}_3$  nanowires.<sup>14</sup> Fig. 3b shows the dependences of the photocurrent on the power density of incident light at 1 V, 5 V and 10 V, respectively. Usually, the relationship can be described by a power law ( $I_{ph} = A \times P^C$ ,  $I_{ph}$  is photocurrent,  $P$  is power density,  $A$  and  $C$  are constants). The solid lines are the best fitting results. The  $C$  values correspond to 0.82, 0.59 and 0.57, respectively. They are

smaller than 1, indicating that multiple trap states exist in a single  $\text{Sb}_2\text{Se}_3$  nanowire and lead to a complex process of electron-hole generation, trapping and recombination under the illumination.<sup>1,3</sup> The time responses of the single  $\text{Sb}_2\text{Se}_3$  nanowire were recorded by periodically turning 635 nm light on and off, as shown in Fig. 3c,d. It is noted that the photocurrents are stable and reversible. The rise time (fall time) is defined as the time interval for the response to rise (decay) from 10-90 % (90-10 %) of photocurrent. The single  $\text{Sb}_2\text{Se}_3$  nanowire photodetector has the rise/fall time of 2.2/3.7 s, 0.6/3.1 s and 0.4/1.3 s at a bias of 1 V, 5 V and 10 V, respectively. These response times are comparable to those of  $\text{Sb}_2\text{Se}_3$  nanowire photodetectors and other nanowire photodetectors.<sup>29,33,34</sup> There are rare dangling bonds on the surface of  $\text{Sb}_2\text{Se}_3$  nanowires due to the layered structure.<sup>30</sup> Less dangling bonds indicate less surface states in the surface region. It has been known that a long response time is due to the existence of a large amount of surface states, and vice versa.<sup>35</sup> Thus, the fast response to 635 nm light should be attributed to the layered structure of  $\text{Sb}_2\text{Se}_3$ . It is also observed that the response time can be shortened by increasing the bias. Increasing the bias can enhance the strength of the electric field in the nanowire, which could accelerate the trapping and releasing process of carriers and finally lead to a fast response. In addition, the fall time is longer than the rise time at a fixed bias.

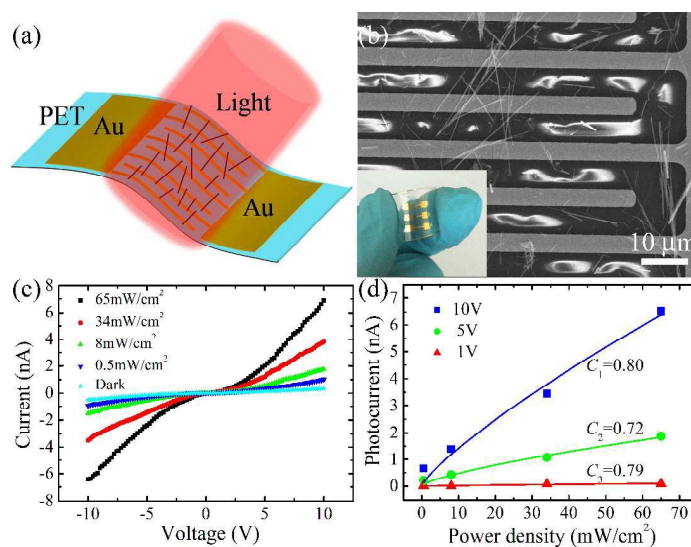


**Fig. 4** (a) Schematic illustration and (b) SEM image of a flexible photodetector based on multiple  $\text{Sb}_2\text{Se}_3$  nanowires. Inset shows three pairs of interdigitated electrodes on the flexible PET substrate. (c)  $I$ - $V$  curves of the photodetector (D1) in the dark and under the illumination of 635 nm light. (d) The relationships between photocurrent and power density.

The fabrication process of single nanowire based photodetectors is complex, expensive and time consuming. Moreover, single nanowire's photocurrent is too small to be detected. Thus, single nanowire based photodetectors are hard to be used widely in daily life. Recently, flexible electronics have attracted more attention due to the demand for portable devices. In this work, a large number of  $\text{Sb}_2\text{Se}_3$  nanowires were randomly dispersed onto the Au interdigitated electrodes on PET substrates to fabricate flexible photodetectors. Fig. 4a is a schematic illustration of flexible photodetector. Because the Au interdigitated electrodes are made on the flexible PET substrate, as shown in the inset of Fig. 4b, the photodetector could possess excellent

flexibility. A flexible photodetector was characterized by SEM (Fig. 4b). It is observed that many  $\text{Sb}_2\text{Se}_3$  nanowires are on the interdigitated electrodes and connect adjacent electrodes. As the PET substrate is insulating, there are some bright areas between electrodes induced by the charging effect. Fig. 4c reveals  $I$ - $V$  characteristics of a multiple  $\text{Sb}_2\text{Se}_3$  nanowires based photodetector (D1) in the dark and under the illumination of 635 nm light with different power densities. The photocurrent increases by increasing the power density of incident light at a fixed bias, and their relationships are shown in Fig. 4d. Similarly, the relationships still can be described by the power law ( $I_{ph}=A \times P^C$ ).  $C$  values are taken by fitting corresponding data and are 0.79, 0.72 and 0.80 at a bias of 1 V, 5 V and 10 V, respectively. These values are different from those of the single  $\text{Sb}_2\text{Se}_3$  nanowire photodetector, which is attributed to the difference of electron-hole generation, trapping and recombination processes in two kinds of photodetectors. It is possible that interfaces among nanowires lead to this difference. It is desired to achieve photodetectors of a higher  $C$  value.<sup>32</sup> Compared to the single  $\text{Sb}_2\text{Se}_3$  nanowire based photodetector, the multiple nanowires based photodetector has higher  $C$  values at 5 V, 10 V and a similar value at 1 V.

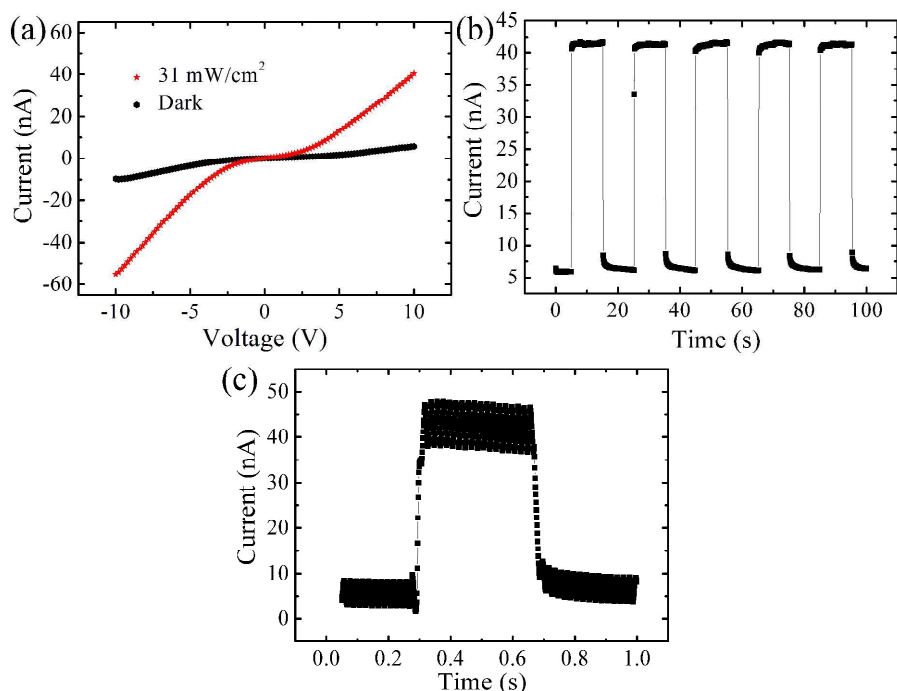


**Fig. 5** (a)  $I-V$  curves of another flexible photodetector (D2) in the dark and under the illumination of 31 mW/cm<sup>2</sup> 635 nm light. (b,c) The time responses to 31 mW/cm<sup>2</sup> 635 nm light at a bias of 10 V with 100 ms and 1 ms time resolutions respectively.

Fig. 5a shows  $I-V$  curves of another flexible Sb<sub>2</sub>Se<sub>3</sub> nanowires based photodetector (D2) in the dark and under the illumination of 31 mW/cm<sup>2</sup> 635 nm light. Compared to D1, the D2 displays a tenfold increase in photocurrent and dark current under the same conditions due to the increasing of the number of nanowires on the interdigitated electrodes. The time responses of the D2 were recorded (Fig. 5b, c). With 635 nm light on and off, the D2 shows “on-state” and “off-state” repeatedly. It has a fast response to the light and a reproducible and stable photocurrent. Fig. 5c illustrates an on-off cycle of the D2 under the illumination of 31 mW/cm<sup>2</sup> 635 nm light at a bias of 10 V with 1 ms time resolution. According to this on-off cycle, it can

be deduced that the rise/fall time is 17/20 ms. In order to confirm the fast response of this kind of flexible photodetectors, the performances of other photodetectors also were characterized. One of them is shown in Fig. S3. The rise/fall time of the DS1 is 13/20 ms and close to 17/20 ms obtained above. Fig. S3c reveals the ability of the DS1 to detect 635 nm light with an on-off frequency up to 230 Hz. The response time is an important parameter determining the capability of photodetector to follow a fast changing light. The response speed of our flexible photodetectors is faster than those of many flexible photodetectors.<sup>15,20,22</sup> Thus, our synthesized  $\text{Sb}_2\text{Se}_3$  nanowires are promising to fabricate high-speed flexible photodetectors. Compared to the single nanowire photodetector, multiple  $\text{Sb}_2\text{Se}_3$  nanowires photodetectors have a faster response speed. Fig. S4 shows that increasing the number of nanowires in the photodetector can improve response speed. The mechanism is still unknown and will be further studied. It is possible that the faster response speed of multiple nanowires photodetector is attributed to the rapid recombination of photogenerated electron-hole pairs at the interfaces between nanowires.<sup>11</sup> Except for 635 nm light, flexible  $\text{Sb}_2\text{Se}_3$  nanowires photodetectors can be used to detect visible-light of other wavelength, such as 405 nm violet light. Fig. S5 illustrates the response of a flexible photodetector to 405 nm light, which is similar to the response to 635 nm light.

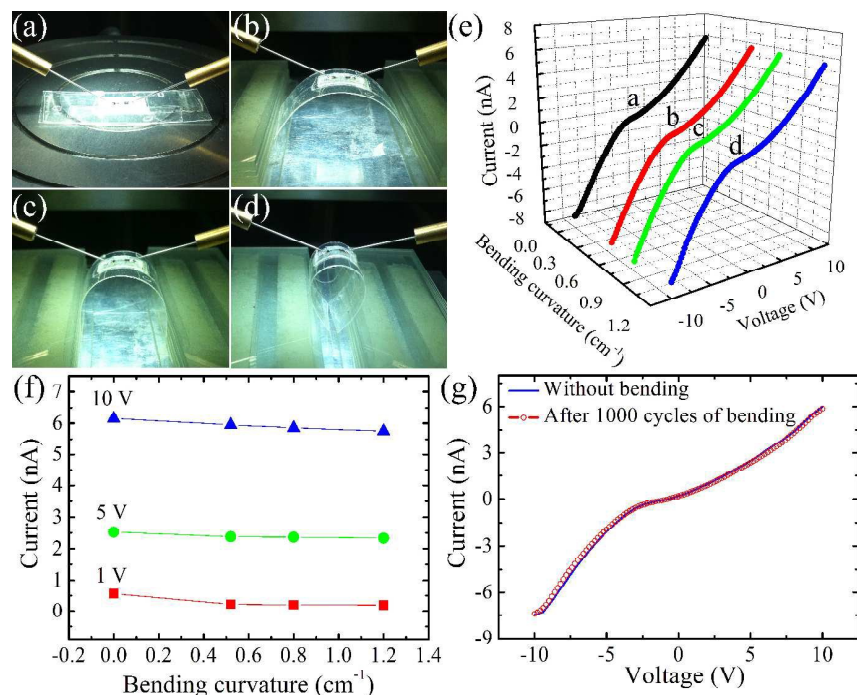


**Fig. 6** (a-d) Photographs show that a flexible photodetector was measured at different bending states. (e)  $I$ - $V$  curves of the flexible photodetector under the white light illumination corresponding to the bending states a-d, respectively. (f) The influence of the bending curvature on the current of the flexible photodetector. (g)  $I$ - $V$  curves measured without bending and after 1000 cycles of bending.

As multiple  $\text{Sb}_2\text{Se}_3$  nanowires photodetectors were fabricated on PET substrates, they should possess a significant property, i.e. flexibility. It is necessary to know the influence of bending on the electrical properties of flexible photodetectors. Fig. 6a-d are photographs recording different bending states of a flexible photodetector during  $I$ - $V$  tests. The corresponding  $I$ - $V$  curves are displayed in Fig. 6e. It is noted that the bending curvature has not an obvious influence on  $I$ - $V$  characteristic of the flexible photodetector. The relationships between the current through the photodetector and

the bending curvature are shown in Fig. 6f. The current slightly decreases with the increasing of bending curvature, which is reasonable since the electrode interspacing should slightly increase with the bending curvature and finally has an influence on the current.<sup>1</sup> However, the currents of the photodetector with different bending curvatures keep at  $6.0 \pm 0.2$  nA. The change of current is negligible and acceptable, indicating the excellent flexibility of this kind of photodetector. Fig. 6g demonstrates  $I$ - $V$  curves of the photodetector without bending (blue solid line) and after 1000 cycles of bending (red circles). It can be observed that  $I$ - $V$  characteristic of the photodetector is hardly affected even after 1000 cycles of bending. All results confirm that dispersing  $\text{Sb}_2\text{Se}_3$  nanowires onto the Au interdigitated electrodes is suitable for making flexible photodetectors with high-performance. Since  $(\text{Sb}_4\text{Se}_6)_n$  layers are parallel to the growth direction of  $\text{Sb}_2\text{Se}_3$  nanowire, the nanowires could have large bending strain compliance. Thus, excellent flexibility should be also related to the layered structure.

Table 1 Comparison of  $\text{Sb}_2\text{Se}_3$  nanostructure based photodetectors

Photodetectors	Response time (s)	Responsivity (A/W)	$EQE$ (%)	Flexibility	Reference
Single $\text{Sb}_2\text{Se}_3$ nanowire		560	$1.06 \times 10^5$	No	27
Single $\text{Sb}_2\text{Se}_3$ nanowire	<0.3 s	8.0	1650	No	29
Multiple $\text{Sb}_2\text{Se}_3$ nanowires	0.2/1.2 s			No	31
Single $\text{Sb}_2\text{Se}_3$ nanowire	0.4/1.3 s	360	$7.0 \times 10^4$	No	This work
Multiple $\text{Sb}_2\text{Se}_3$ nanowires	13/20 ms			Yes	This work

Our results are compared with other  $\text{Sb}_2\text{Se}_3$  nanostructure based photodetectors reported so far (Table 1). In this work, the single  $\text{Sb}_2\text{Se}_3$  nanowire shows an excellent

light-detection performance with high responsivity and fast time response.  $\text{Sb}_2\text{Se}_3$  nanowires can be assembled into a flexible photodetector with faster time response and excellent flexibility by a simple method. This work first reveals that high-yield  $\text{Sb}_2\text{Se}_3$  nanowires are promising candidates for flexible photodetectors.

### Conclusions

High-quality single-crystalline  $\text{Sb}_2\text{Se}_3$  nanowires have been fabricated by a simple hydrothermal method. The conductivity type of  $\text{Sb}_2\text{Se}_3$  nanowires is confirmed as p-type, which is same as that of the bulk. The response of a single  $\text{Sb}_2\text{Se}_3$  nanowire to 635 nm light has been investigated. Its responsivity and EQE are 360 A/W and  $7.0 \times 10^4$  %, respectively. Its rise/fall time is 0.4/1.3 s. A large number of  $\text{Sb}_2\text{Se}_3$  nanowires can be assembled easily into a flexible multiple nanowires based photodetector. This kind of flexible photodetectors has a fast response to 635 nm light with the rise/fall time as low as 13/20 ms. The current through flexible photodetectors remains nearly unchanged at different bending states and after 1000-cycles bending, confirming excellent flexibility. Our results illustrate the promising application of  $\text{Sb}_2\text{Se}_3$  nanowires in high-performance flexible photodetectors.

### Acknowledgements

This work was financially supported by the National Natural Science Foundation of China (Project No. 61204016 and 11104047) and the Program for Excellent Talents in University of Education Bureau of Liaoning Province (LJQ2014047).

**Notes and references**

- 1 Xuming Xie and Guozhen Shen, *Nanoscale*, 2015, **7**, 5046.
- 2 Zhengtao Deng, Di Cao, Jin He, Su Lin, Stuart M. Lindsay and Yan Liu, *ACS Nano*, 2012, **6**, 6197.
- 3 Yao Liang, Hui Liang, Xudong Xiao and Suikong Hark, *J. Mater. Chem.*, 2012, **22**, 1199.
- 4 Wen Dai, Xinhua Pan, Shanshan Chen, Cong Chen, Wei Chen, Honghai Zhang and Zhizhen Ye, *RSC Adv.*, 2015, **5**, 6311.
- 5 Liang Li, Yong Zhang, Xiaosheng Fang, Tianyou Zhai, Meiyong Liao, Xueliang Sun, Yasuo Koide, Yoshio Bando and Dmitri Golberg, *J. Mater. Chem.*, 2011, **21**, 6525.
- 6 Lianbo Wang, Weiyu Yang, Haining Chong, Lin Wang, Fengmei Gao, Linhai Tian and Zuobao Yang, *RSC Adv.*, 2015, **5**, 52388.
- 7 Zhe Liu, Bo Liang, Gui Chen, Gang Yu, Zhong Xie, Lina Gao, Di Chen and Guozhen Shen, *J. Mater. Chem. C*, 2013, **1**, 131.
- 8 Chaoyi Yan, Nandan Singh and Pooi See Lee, *Appl. Phys. Lett.*, 2010, **96**, 053108.
- 9 Cheol-Joo Kim, Hyun-Seung Lee, Yong-Jun Cho, Kibum Kang and Moon-Ho Jo, *Nano Lett.*, 2010, **10**, 2043.
- 10 Tianyou Zhai, Ying Ma, Liang Li, Xiaosheng Fang, Meiyong Liao, Yasuo Koide, Jiannian Yao, Yoshio Bando and Dmitri Golberg, *J. Mater. Chem.*, 2010, **20**, 6630.
- 11 Sheng-Chin Kung, Wytze E. van der Veer, Fan Yang, Keith C. Donovan and Reginald M. Penner, *Nano Lett.*, 2010, **10**, 1481.
- 12 Liang Li, Xiaosheng Fang, Tianyou Zhai, Meiyong Liao, Ujjal K Gautam, Xingcai Wu, Yasuo Koide, Yoshio Bando and Dmitri Golberg, *Adv. Mater.*, 2010, **22**, 4151.

- 13 Peicai Wu, Yu Dai, Yu Ye, Yang Yin and Lun Dai, *J. Mater. Chem.*, 2011, **21**, 2563.
- 14 Wei-Wei Xiong, Jin-Qiang Chen, Xing-Cai Wu and Jun-Jie Zhu, *J. Mater. Chem. C*, 2015, **3**, 1929.
- 15 Gui Chen, Bo Liang, Zhe Liu, Gang Yu, Xuming Xie, Tao Luo, Zhong Xie, Di Chen, Ming-Qiang Zhu and Guozhen Shen, *J. Mater. Chem. C*, 2014, **2**, 1270.
- 16 Lin-Bao Luo, Xiao-Bao Yang, Feng-Xia Liang, Jian-Sheng Jie, Qiang Li, Zhi-Feng Zhu, Chun-Yan Wu, Yong-Qiang Yu and Li Wang, *CrystEngComm*, 2012, **14**, 1942.
- 17 Hahn-Gil Cheong, Ross. E. Triambulo, Gun-Hwan Lee, In-Sook Yi and Jin-Woo Park, *ACS Appl. Mater. Interfaces*, 2014, **6**, 7846.
- 18 Xianfu Wang , Xihong Lu , Bin Liu , Di Chen , Yexiang Tong and Guozhen Shen, *Adv. Mater.*, 2014, **26**, 4763–4782.
- 19 Yuan Liu, Hailong Zhou, Rui Cheng, Woojong Yu, Yu Huang and Xiangfeng Duan, *Nano Lett.*, 2014, **14**, 1413.
- 20 Gang Yu, Zhe Liu, Xuming Xie, Xia Ouyang and Guozhen Shen, *J. Mater. Chem. C*, 2014, **2**, 6104.
- 21 Suo Bai, Weiwei Wu, Yong Qin, Nuanyang Cui, Dylan J. Bayerl and Xudong Wang, *Adv. Funct. Mater.*, 2011, **21**, 4464.
- 22 Jiangxin Wang, Chaoyi Yan, Meng-Fang Lin, Kazuhito Tsukagoshi and Pooi See Lee, *J. Mater. Chem. C*, 2015, **3**, 596.
- 23 Hao Wu, Zheng Lou, Hong Yang and Guozhen Shen, *Nanoscale*, 2015, **7**, 1921.
- 24 Rencheng Jin, Gang Chen, Jian Pei, Jingxue Sun and Yang Wang, *Nanoscale*, 2011, **3**, 3893.

- 25 Jianmin Ma, Yaping Wang, Yijing Wang, Peng Peng, Jiabiao Lian, Xiaochuan Duan, Zhifang Liu, Xiaodi Liu, Qing Chen, Tongil Kim, Gang Yao and Wenjun Zheng, *CrystEngComm*, 2011, **13**, 2369.
- 26 Rencheng Jin, Gang Chen, Qun Wang, Jingxue Sun and Yang Wang, *J. Mater. Chem.*, 2011, **21**, 6628.
- 27 Donghyeuk Choi, Yamujin Jang, JeeHee Lee, Gyoung Hwa Jeong, Dongmok Whang, Sung Woo Hwang, Kyung-Sang Cho and Sang-Wook Kim, *Sci. Rep.*, 2014, **4**, 6714.
- 28 Jianmin Ma, Yaping Wang, Yijing Wang, Qing Chen, Jiabiao Lian and Wenjun Zheng, *J. Phys. Chem. C*, 2009, **113**, 13588.
- 29 Tianyou Zhai, Mingfu Ye, Liang Li, Xiaosheng Fang, Meiyong Liao, Yongfang Li, Yasuo Koide, Yoshio Bando and Dmitri Golberg, *Adv. Mater.*, 2010, **22**, 4530.
- 30 Ying Zhou, Liang Wang, Shiyu Chen, Sikai Qin, Xinsheng Liu, Jie Chen, Ding-Jiang Xue, Miao Luo, Yuanzhi Cao, Yibing Cheng, Edward H. Sargent and Jiang Tang, *Nature Photonics*, 2015, **9**, 409.
- 31 Yong-Qiang Liu, Meng Zhang, Feng-Xia Wang and Ge-Bo Pan, *J. Mater. Chem. C*, 2014, **2**, 240.
- 32 Zhenxing Wang, Muhammad Safdar, Misbah Mirza, Kai Xu, Qisheng Wang, Yun Huang, Fengmei Wang, Xueying Zhan and Jun He, *Nanoscale*, 2015, **7**, 7252.
- 33 Junfeng Lu, Chunxiang Xu, Jun Dai, Jitao Li, Yueyue Wang, Yi Lin and Panlin Li, *Nanoscale*, 2015, **7**, 3396.

- 34 Tianyou Zhai, Xiaosheng Fang, Meiyong Liao, Xijin Xu, Liang Li, Baodan Liu, Yasuo Koide, Ying Ma, Jiannian Yao, Yoshio Bando and Dmitri Golberg, *ACS Nano*, 2010, **4**, 1596.
- 35 Xing Xie, So-Ying Kwok, Zhenzhen Lu, Yankuan Liu, Yulin Cao, Linbao Luo, J. A. Zapien, Igor Bello, Chun-Sing Lee, Shuit-Tong Lee and Wenjun Zhang, *Nanoscale*, 2012, **4**, 2914.

## Graphical Abstract

Flexible visible-light photodetectors were fabricated by dispersing a large number of  $\text{Sb}_2\text{Se}_3$  nanowires onto the Au interdigitated electrodes on PET substrates, which showed fast response speed and excellent flexibility.

